Synthesis of Transition-Metal-Incorporated Nickel Phosphate Molecular Sieves TMI−VSB-1

Sung Hwa Jhung,[†] Jong-San Chang,*[,†] Ji Woong Yoon,[†] Jean-Marc Grenèche,[‡] Gérard Férey,[§] and Anthony K. Cheetham*[,∥]

Research Center for Nanocatalysis, Korea Research Institute of Chemical Technology, P.O. Box 107, Yusung, Daejeon 305-600, Korea, Laboratoire de Physique de l'Etat Condensé, Université du Maine, 72000 Le Mans, France, Institut Lavoisier, UMR CNRS 173, Université de Versailles Saint Quentin, 45 avenue des Etats-Unis, 78035 Versailles Cedex, France, and Materials Research Laboratory, University of California, Santa Barbara, California 93106-5121

Received June 8, 2004
Revised Manuscript Received August 31, 2004

Isomorphous incorporation of transition metal ions (TMI) in the framework of porous materials such as zeolites and aluminophosphate (AlPO) molecular sieves has attracted considerable attention[1,2] because metal-incorporated molecular sieves contain atomically dispersed metal species that may impart novel catalytic and adsorptive properties.[3] However, for metal-incorporated AlPO molecular sieves (MeAPO-*n*), it has been difficult to verify metal incorporation into the framework by typical characterization methods. Despite significant differences in bond length between TMI−O and Al−O or P−O, the amount of incorporated transition metal ions is normally insufficient[2] to change the unit cell (UC) dimensions beyond experimental error. Despite a few studies verifying the metal substitution by XAS/XRD[4] and ESEM,[5] it is still debated whether the substitution site for TMI is at the Al or P sites in certain MeAPO-*n* materials.[2]

We recently discovered two different nanoporous nickel(II) phosphates, VSB-1 and VSB-5, with interesting catalytic and adsorption properties.[6,7] The structure of VSB-1 is based on a 3D network of octahedral (O_h) Ni and tetrahedral (T_d) P defining a large, unidimensional channel.[6] It is important to note that the framework nickel atoms have octahedral coordination in the VSB-1 structure, and are thus different from those incorporated into AlPO and SAPO molecular sieves which are tetrahedrally coordinated (for example, Ni−SAPO-34[8]). In this communication, we report the isomorphous substitution of various TMIs into the VSB-1 framework, as confirmed by the change of UC dimensions and chemical and spectroscopic analysis. We have also investigated the preferred coordination geometries of the TMIs substituted into VSB-1.

The VSB-1 and transition metal ion-incorporated VSB-1 (TMI−VSB-1) materials were synthesized under microwave irradiation using the apparatus described previously.[9] We adopted microwave synthesis because it has been applied to the fast crystallization of inorganic porous materials so that various reaction parameters can be easily examined.[9,10] The synthesis was carried out at 180 °C for 1 h in acidic conditions without any organic template.[11] The reactant composition was *x*:1.0:1.0:2.5:100 TMI/H_3PO_4/$NiCl_2$/NH_4F/H_2O. The atomic concentration of added or incorporated TMI is reported in atomic % based on total concentration of TMI, Ni, and P. The precursors for Fe, V, Zn, and Co were $FeCl_2 \cdot 4H_2O$, $VOSO_4 \cdot 4H_2O$, $Zn(NO_3)_2 \cdot 6H_2O$, and $Co(OAc)_2 \cdot 4H_2O$, respectively. The UC dimensions were calculated using a standard least squares refinement program[12] and α-alumina was used as an internal standard. The UV/Vis diffuse reflectance spectra (UV/Vis-DRS) were recorded under ambient condition using an UV/Vis spectrophometer equipped with a quartz cell. The chemical compositions of the as-synthesized materials were determined by ICP analysis. Mössbauer experiments for iron were performed at both 300 and 77 K using a constant acceleration mode spectrometer and a ^{57}Co source diffused into a Rh matrix. The values of isomer shift are quoted relative to α-Fe at 300 K.

The synthesized VSB-1 and TMI−VSB-1 molecular sieves are highly crystalline and have homogeneous morphologies as shown by the XRD patterns (data not shown) and SEM images (Supporting Information Figure 1). The aspect ratio increases substantially with the incorporation of TMIs such as iron, vanadium, and cobalt. The chemical compositions of Fe−VSB-1 are summarized in Table 1.

[†] Korea Research Institute of Chemical Technology.
[‡] Université du Maine.
[§] Université de Versailles Saint Quentin.
[∥] University of California, Santa Barbara.

(1) Hartmann, M.; Kevan, L. *Chem. Rev.* **1999**, *99*, 635, and references therein.
(2) Weckhuysen, B. M.; Rao, R. R.; Martens, J. A.; Schoonheydt, R. A. *Eur. J. Inorg. Chem*. **1999**, 565, and references therein.
(3) (a) De Vos, D. E.; Sels, B. F.; Jacobs, P. A. *Adv. Synth. Catal.* **2003**, *345*, 457, and references therein. (b) Panov, G. I. *CATTECH* **2000**, *4*, 18, and references therein. (c) Thomas, J. M.; Raja, R.; Sankar, G.; Bell, R. G. *Acc. Chem. Res.* **2001**, *34*, 191, and references therein. (d) Davis, M. E. *Nature* **2002**, *417*, 813, and references therein. (e) Matsuoka, M.; Anpo, M. *J. Photochem. Photobiol., C* **2003**, *3*, 225, and references therein.
(4) Thomas, J. M. *Angew. Chem., Int. Ed.* **1999**, *38*, 3588.
(5) Prakash, A. M.; Hartmann, M.; Zhu, Z.; Kevan, L. *J. Phys. Chem. B* **2000**, *104*, 1610.
(6) (a) Guillou, N.; Gao, Q.; Nogues, M.; Morris, R. E.; Hervieu, M.; Férey, G.; Cheetham, A. K. *Acad. Sci. Paris* **1999**, *2*, 387. (b) Chang, J.-S.; Park, S.-E.; Gao, Q.; Férey, G.; Cheetham, A. K. *Chem. Commun.* **2001**, 859. (c) Chang, J.-S.; Hwang, J.-S.; Jhung, S. H.; Park, S.-E.; Férey, G.; Cheetham, A. K. *Angew. Chem., Intl. Ed.* **2004**, *43*, 2819.
(7) (a) Guillou, N.; Gao, Q.; Forster, P. M.; Chang, J.-S.; Noguès, M.; Park, S.-E.; Férey, G.; Cheetham, A. K. *Angew. Chem., Int. Ed.* **2001**, *40*, 2831. (b) Forster, P. M.; Eckert, J.; Chang, J.-S.; Park, S.-E.; Férey, G.; Cheetham, A. K. *J. Am. Chem. Soc.* **2003**, *125*, 1309. (c) Jhung, S. H.; Chang, J.-S.; Park, S.-E.; Forster, P. M.; Férey, G.; Cheetham, A. K. *Chem. Mater.* **2004**, *16*, 1394.
(8) Inoue, M.; Dhupatemiya, P.; Phatanasri, S.; Inui, T. T. *Microporous Mesoporous Mater.* **1999**, *28*, 19.
(9) (a) Park, S.-E.; Chang, J.-S.; Hwang, Y. K.; Kim, D. S.; Jhung, S. H.; Hwang, J. S. *Catal. Surv. Asia* **2004**, *8*, 91, and references therein. (b) Jhung, S. H.; Chang, J.-S.; Hwang, Y. K.; Park, S.-E. *J. Mater. Chem.* **2004**, *14*, 280.
(10) (a) Rao, K. J.; Vaidhyanathan, B.; Ganguli, M.; Ramakrishnan, P. A. *Chem. Mater.* **1999**, *11*, 882, and references therein. (b) Cundy, C. S.; Plaisted, R. J.; Zhao, J. P. *Chem. Commun.* **1998**, 1465.
(11) VSB-1 can be obtained without any template under suitable pH of 2.5−5.0. Jhung, S. H.; Chang, J.-S.; et al. Manuscript in preparation.
(12) Holland, T. J. B.; Redfern, S. A. T. *J. Appl. Crystallogr.* **1997**, *30*, 84.

10.1021/cm049081e CCC: $27.50
Published on Web 11/24/2004

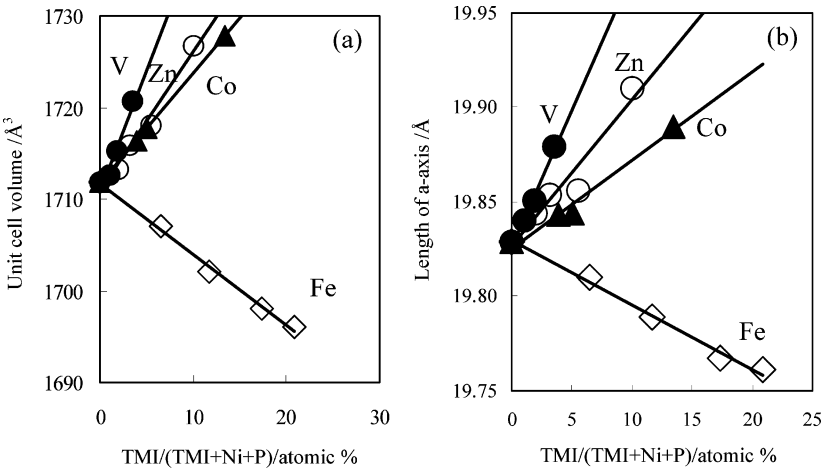

Figure 1. Changes of (a) UC volume and (b) the length of *a*-axis of the TMI−VSB-1 materials according to the type of TMI and concentration of TMI incorporated. The size of symbol corresponds approximately to the experimental error.

Table 1. Chemical Compositions of Reaction Mixtures and the As-Synthesized Fe−VSB-1 Materials

	relative composition of reaction mixture for Fe−VSB-1 (atomic %)[a]			normalized compositions of as-synthesized Fe−VSB-1 (atomic %, ± 0.3)[a]		
sample	Fe	Ni	P	Fe	Ni	P
A	0.0	50.0	50.0	0.0	56.2	43.8
B	5.0	47.5	47.5	6.5	50.1	43.4
C	10.0	45.0	45.0	11.7	45.1	43.2
D	15.0	42.5	42.5	17.3	39.3	43.4
E	20.0	40.0	40.0	20.9	36.3	42.8

[a] Based only on the concentration of Fe, Ni, and P.

The change of UC parameters upon metal incorporation without changing crystal symmetry of the host structure provides direct evidence of the isomorphous substitution. As expected, the incorporation of TMIs into the VSB-1 framework leads to an increase or decrease in UC volumes of the crystal structure depending on the identity of the TMI. UC volumes and *a*-axis lengths of TMI−VSB-1 increase due to substitution for all elements studied except Fe−VSB-1, where the UC parameters contract with increasing iron substitution (Figure 1). However, the change of *c*-axis length upon metal incorporation depends on the type of metal ions (Supporting Information Figure 2). Interestingly, the *c*-axis does not change with V concentration in V−VSB-1 similar to the result of VAPO-5.[13] It is not yet clear why a change of the *c*-axis length is not sensitive to V concentration in V−VSB-1, but it is thought that the peculiarity of vanadium is probably related to the presence of vanadyl groups in the framework that are usually observed in VAPO-*n*.[1,2] Detailed study is necessary to understand effects of type of TMIs on *c*-axis length.

It has already been pointed out[2,14] that the formal charge and ionic radius of the TMI are very important factors in determining the level of isomorphous substitution of the TMI into a molecular sieve. Based on the data of Shannon,[15] the observed increases of UC

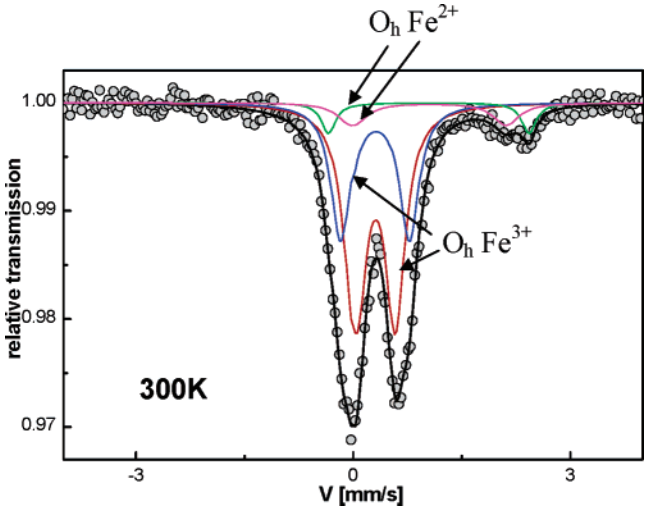

Figure 2. Mössbauer spectrum of Fe−VSB-1 (Sample E) at 300 K fitted with four quadrupolar doublets. The two contributions of both O_h Fe^{3+} and O_h Fe^{2+} are shown. The relative contents of Fe^{3+} and Fe^{2+} in Fe−VSB-1 (Sample E) can be assigned to 87% and 13%, respectively, according to this spectrum.

($UC_{Zn-VSB-1}$ and $UC_{Co-VSB-1} > UC_{VSB-1}$) (Figure 1) are consistent with the ionic radii of these TMI in 6-fold coordination ($R_{Zn}^{2+} > R_{Ni}^{2+}$ and $R_{Co}^{2+} > R_{Ni}^{2+}$). On the contrary, the variations of UC for Fe−VSB-1 and V−VSB-1 are not in agreement with these expectations. Indeed, the volume decreases with Fe whereas $R_{Fe}^{2+} > R_{Ni}^{2+}$ and increases with vanadium whereas $R_V^{4+} < R_{Ni}^{2+}$.

Concerning Fe−VSB-1, it is well-known that in acidic medium, Fe^{2+} ($R_{Fe}^{2+} = 0.78$ Å in O_h coordination) tends to be oxidized into Fe^{3+} ($R_{Fe}^{3+} = 0.645$ Å in the same coordination).[2,16] As the synthesis conditions correspond to acidic conditions, such a process could explain the corresponding decrease of the cell volume. Our Mössbauer results confirm the oxidation of about 90% of the Fe^{2+} to Fe^{3+} and the coordination of iron to be octahedral. Figure 2 illustrates the Mössbauer spectrum recorded at 300 K on Fe−VSB-5 (Sample E), while Table 2 summarizes the refined values of the Mössbauer

(13) Blasco, T.; Concepcióén, P.; Nieto, J. M.; Prez-Pariente, J. *J. Catal.* **1995**, *152*, 1.
(14) (a) Martens, J. A.; Jacobs, P. A. *Stud. Surf. Sci. Catal.* **1994**, *85*, 653, and references therein. (b) Wilson, S. T. *Stud. Surf. Sci. Catal.* **2001**, *137*, 229, and references therein. (c) Feng, P.; Bu, X.; Stucky, G. D. *Nature* **1997**, *388*, 735.
(15) Shannon, R. *Acta Crystallogr.* **1976**, *A32*, 751.
(16) Risteć, A.; Tušar, N. N.; Arčon, I.; Zabukovec, N.; Thibault-Starzyk, F.; Czyzniewska, J.; Kaučič, V. *Chem. Mater.* **2003**, *15*, 3643.

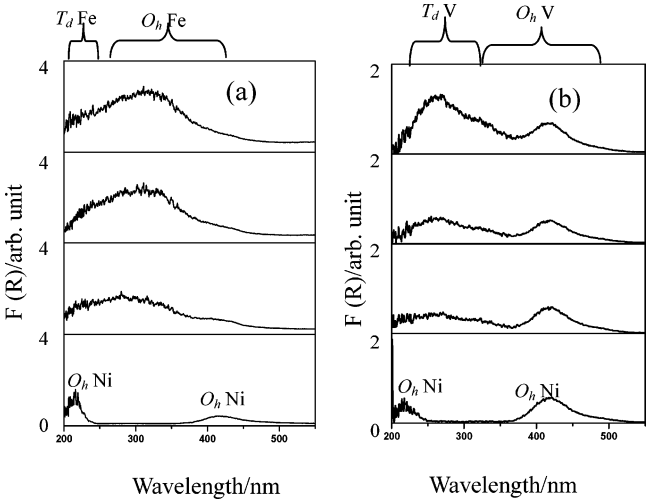

Figure 3. UV/Vis-DRS spectra of (a) Fe−VSB-1 and (b) V−VSB-1 according to the concentration of incorporated metal ions. The concentration of TMI increases from bottom to top. The lowest spectra correspond to that of VSB-1 without any TMI.

Table 2. Refined Fitting Parameters for the Mössbauer Spectra of Fe−VSB-1 (Sample E)[a]

temp.	IS (mm/s) ± 0.01	Γ (mm/s) ± 0.01	Δ (mm/s) ± 0.02	assigned species	proportion (%) ± 1
300 K	0.42	0.33	0.54	Fe^{3+} (O_h)	44
	0.43	0.32	0.92	Fe^{3+} (O_h)	43
	1.17	0.24	2.74	Fe^{2+} (O_h)	6
	1.17	0.24	2.11	Fe^{2+} (O_h)	7
77 K	0.53	0.32	0.54	Fe^{3+} (O_h)	45
	0.54	0.36	0.90	Fe^{3+} (O_h)	41
	1.36	0.34	3.06	Fe^{2+} (O_h)	14

[a] IS, Γ, and Δ correspond to isomer shift quoted relative to that of α-Fe at 300 K, linewidth at half-height, and quadrupolar splitting, respectively.

parameters from the spectra at 77 and 300 K. One clearly observes a prevailing quadrupolar doublet with a small asymmetry, located at the low velocity range and a single line at about 3 mm/s. The spectrum can be refined with three quadrupolar doublets and four quadrupolar doublets at 77 and 300 K, respectively.[17] Thanks to the values of isomer shift, the first two quadrupolar doublets are unambiguously attributed to high-spin Fe^{3+} located in FeO_6 octahedral units, while the third quadrupolar doublet at 77 K and the last two ones at 300 K are clearly attributed to high-spin Fe^{2+} ions with octahedral coordination. In addition, this study provides the content of both Fe^{3+} and Fe^{2+} in this mixed valence compound as listed in Table 2. One has to note that the values at 300 K are similar to those at 77 K. Moreover, other Fe−VSB-1s with lower iron contents consist of approximately 90% Fe $^{3+}$ and 10% Fe $^{2+}$ (data not shown).[17]

The mean radius (0.659 Å) corresponding to this occupancy (90% Fe^{3+} and 10% Fe^{2+}) is then consistent with the observed decrease in UC volume ($R_{Ni}^{2+} = 0.69$ Å). The substitution mechanism is also confirmed by the UV/Vis-DRS analysis (Figure 3). The UV absorption bands due to charge transfer of octahedral Fe^{3+} are known to occur around 278 nm for isolated Fe^{3+}, 333 nm for small clusters, and 427 nm for Fe_2O_3, compared with around 215 ($t_1 \rightarrow t_2$) and 241 nm ($t_1 \rightarrow e$ transition) for tetrahedral Fe^{3+}.[18] The UV/Vis-DRS spectra of Fe−VSB-1 show very broad bands in the range 200−400 nm, quite different from those of $Fe^{3+}(T_d)$ present in Fe−ZSM-5, which exhibit a maximum of absorption below 225 nm. These results strongly suggest that the Fe^{3+} ions in Fe−VSB-1 principally substitute at the octahedral nickel sites.

The substitution site for Fe can also be verified by chemical analysis (ICP), as shown in Table 1. The chemical compositions of the Fe−VSB-1 materials exhibit a steady decrease of Ni concentration with increasing Fe concentration, demonstrating that the Fe ions are isomorphously incorporated into the Ni sites in VSB-1. However, a small amount of extraframework iron species may exist considering the slight decrease of phosphorus concentration with increasing iron concentration.

On the basis of the same interpretation as above, an increase of UC volume with increasing vanadium concentration in VSB-1 cannot be explained by the substitution of nickel with V^{4+} because $R_V^{4+} < R_{Ni}^{2+}$. Indeed, the increase of UC of V−VSB-1 may be explained with the replacement of P^{5+} by V^{4+} because $R_V^{4+} > R_P^{5+}$. It is also noticeable that the dependences of the UC volume with the incorporation of TMI (slope of Figure 1) rely on the difference of ionic radii: $(R_V^{4+} - R_P^{5+}) > (R_{Zn}^{2+} - R_{Ni}^{2+}) > (R_{Co}^{2+} - R_{Ni}^{2+}) > (R_{Fe}^{3+/2+} - R_{Ni}^{2+})$.

Moreover, the substitution of phosphorus with vanadium may be confirmed by the T_d symmetry of the vanadium species in V−VSB-1. The UV absorptions for vanadium are reported to be[13,19] 250−286 nm for $V^{4+}(T_d)$, 286−333 nm for $V^{5+}(T_d)$, and 330−500 nm for $V^{5+}(O_h)$. The experimental absorption spectra (Figure 3) are mainly in favor of the major existence of tetrahedral V^{4+} though we cannot rule out the presence of tetrahedral V^{5+}, which is also larger than P^{5+}. This means that vanadium principally substitutes for tetrahedral phosphorus sites in the framework of VSB-1, in agreement with the increase of UC volume. However, the substitution mechanism cannot be confirmed by the ICP results to show a steady decrease of nickel and phosphorus concentrations with increasing vanadium concentration. This inconsistency may come from a low level of V incorporation and the contribution of nonframework V species that may exist in small concentration.

For Zn− and Co−VSB-1, chemical analysis results indicate that Zn and Co ions might be incorporated in the Ni sites in VSB-1 (data not shown), in agreement with the UC volume changes ($R_{Ni}^{2+} < R_{Zn}^{2+}$ and $R_{Ni}^{2+} < R_{Co}^{2+}$).

In summary, the isomorphous substitution of various transition metal ions with not only tetrahedral (in the P sites) but also octahedral symmetry (in the Ni sites) in VSB-1 is clearly confirmed by UC parameters, and spectroscopic and chemical analysis. This work demon-

(17) Grenèche, J.-M.; Jhung, S. H.; Chang, J.-S.; et al. Manuscript in preparation.

(18) Bordiga, S.; Buzzoni, R.; Geobaldo, F.; Lamberti, C.; Giamello, E.; Zecchina, A.; Leofanti, G.; Petrini, G.; Tozzola, G.; Vlaic, G. *J. Catal.* **1996**, *158*, 486.

(19) (a) Centi, G.; Perathoner, S.; Trifiró, F.; Aboukais, A.; Aïssi, C. F.; Guelton, M. *J. Phys. Chem.* **1992**, *96*, 2617. (b) Dzwigaj, S.; Matsuoka, M.; Anpo, M.; Che, M. *J. Phys. Chem. B* **2000**, *104*, 6012. (c) Jhung, S. H.; Uh, Y. S.; Chon, H. *Appl. Catal.* **1990**, *62*, 61.

strates that nanoporous VSB-1 has an unusually versatile framework that will accommodate high concentrations (up to 21% for Fe) of various TMIs in comparison with other known zeolitic materials.

Acknowledgment. This work was supported by the Core Nanotechnology Program (Research Center for Nanocatalysis) and the International Collaboration Project of the Korean Ministry of Science and Technology and the MRSEC Program of the National Science Foundation under Award DMR00-80034. We thank Prof. S.-E. Park, Dr. J. S. Yoo, Dr. Y. K. Hwang and Mr. P. M. Forster for valuable discussions.

Supporting Information Available: SEM images of representative samples and graph of changes of UC dimension (length of *c*-axis) with type and concentration of incorporated TMIs. This material is available free of charge via the Internet at http://pubs.acs.org.

CM049081E